

Lightweight Multiscale Feature Fusion Super-Resolution Network Based on Two-branch Convolution and Transformer

Ke Li¹, Yukai Liu¹

¹North China Electric Power University

Abstract—The single image super-resolution(SISR) algorithms under deep learning currently have two main models, one based on convolutional neural networks and the other based on Transformer. The former uses the stacking of convolutional layers with different convolutional kernel sizes to design the model, which enables the model to better extract the local features of the image; the latter uses the self-attention mechanism to design the model, which allows the model to establish long-distance dependencies between image pixel points through the self-attention mechanism and then better extract the global features of the image. However, both of the above methods face their problems. Based on this, this paper proposes a new lightweight multi-scale feature fusion network model based on two-way complementary convolutional and Transformer, which integrates the respective features of Transformer and convolutional neural networks through a two-branch network architecture, to realize the mutual fusion of global and local information. Meanwhile, considering the partial loss of information caused by the low-pixel images trained by the deep neural network, this paper designs a modular connection method of multi-stage feature supplementation to fuse the feature maps extracted from the shallow stage of the model with those extracted from the deep stage of the model, to minimize the loss of the information in the feature images that is beneficial to the image restoration as much as possible, to facilitate the obtaining of a higher-quality restored image. The practical results finally show that the model proposed in this paper is optimal in $\times 2$, $\times 3$ and $\times 4$ image recovery performance when compared with other lightweight models with the same amount of parameters.

I. INTRODUCTION

THE Single Image Super-Resolution(SISR) problem [1] is a classical problem in the field of Image Super-Resolution. The goal of this field is to reconstruct and recover an image from a given low-resolution image to obtain a corresponding high-resolution image. Currently, this technique has been widely used in medical imaging [2], remote sensing [3] [4], video surveillance [5] and other image fields [6]. Research on image super-resolution has made profound developments in recent years, and deep learning-based image super-resolution algorithms are now widely used in single-image super-resolution tasks. The main advantage of the deep learning-based super-resolution algorithm is that it no longer needs to artificially process the data features in the early stage, but makes the model learn the mapping function between LR and HR in an end-to-end way, which substantially improves the performance of the relevant SISR model. In the early days of deep learning applied to the image super-resolution problem, firstly since the work of Dong et al [7]. Convolutional

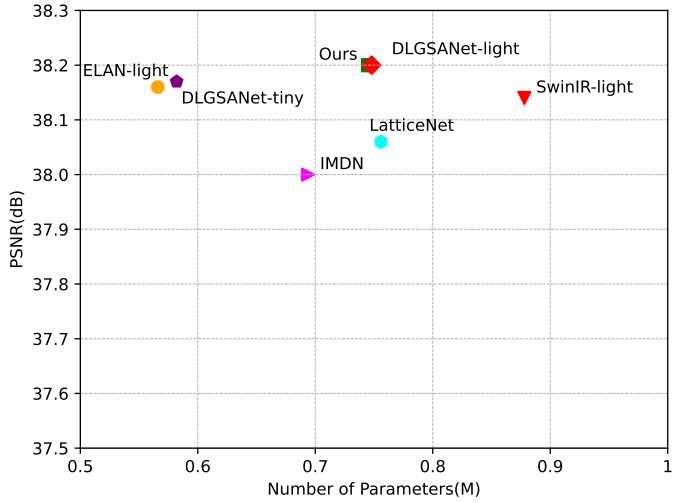


Fig. 1: Visual comparison of other models with our model in terms of number of parameters and PSNR values

Neural Networks were mainly used for the image super-resolution task. However, the main problem with SISR models using convolutional neural networks is that the performance of the convolutional neural network is heavily dependent on the size of the model itself, i.e., the number of parameters and the amount of computation in the model itself. To further improve and enhance the performance of convolutional neural networks, the only way is usually to increase the network size and depth of the model. However, models with too large parameters are more demanding on the hardware devices they are deployed on, requiring strong computational and storage capabilities of the corresponding devices. Therefore models with too large network size are difficult to deploy on non-specialised devices for training. This situation is a great challenge for individuals, enterprises or research institutes that lack computational resources. Therefore, it is necessary to investigate how to lighten the image super-resolution model to reduce the number of model parameters and computation while maintaining a balance with the model performance.

In addition to this, as Transformer has achieved great success in many tasks in the field of Natural Language Processing in recent years, it has prompted people to migrate Transformer, especially techniques such as attention mechanisms, to the field of computer vision [8]. In this context, Liu et al [9].

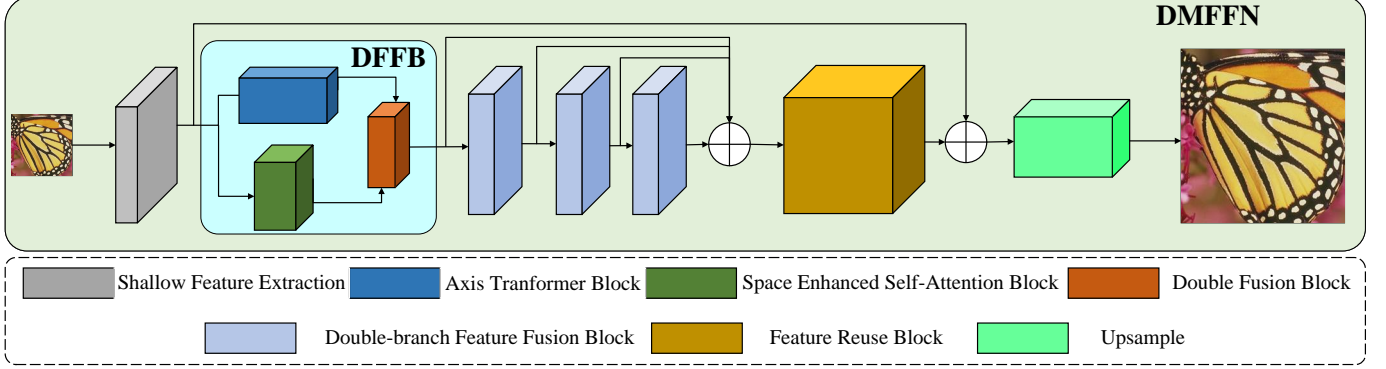


Fig. 2: Main framework of DMFFN

proposed the Swin Transformer model, which has been widely applied to computer vision tasks due to its excellent performance. The Swin Transformer model firstly slices the image by slicing the window, then uses relative position encoding or absolute position encoding between the windows and uses the Shifting Window technique to encode the position of the window on the image. Window) technique to perform multi-level self-attention computation on the image for differently positioned windows, giving the Transformer the ability to establish long-distance pixel dependencies on the image as well. This technique enables the Transformer model to achieve performance beyond that of convolutional neural networks on computer vision tasks.

Although the Swin Transformer model has achieved great success in the field of computer vision, it still suffers from a drawback: the self-attention computation performed by the model inside the window is only local attention, and the establishment of global dependence between image pixels depends on the moving distance of the same window [10] concerning the image between different layers of the network model. Therefore, the image super-resolution network designed based on the Swin Transformer model for a small number of parameters and few network layers is unable to effectively establish a global dependency on the target image, and thus the performance still has a lot of room for improvement.

So in the design process of a lightweight single-image super-resolution network, it is difficult to use a single convolutional neural network or Transformer to achieve the performance of image recovery that people want. To solve the above problems, this paper designs a lightweight single-image super-resolution network based on dual paths, where one branch uses Transformer to extract local and regional features from the image, and one branch uses a convolutional neural network consisting of depth-separable convolutions and combines the channel attention module and spatially-enhanced attention module to extract global coarse-grained features from the image. The network interacts with the information of the features extracted by each of the two branches in the intermediate stage of the model, so that the feature maps after the information interaction retain sufficient information conducive to image recovery, thus achieving the purpose of improving the model's image recovery and image reconstruction capabilities.

On the fusion of two-way features, this paper proposes a fusion module based on multi-scale convolution. In this module by inputting the features to different convolutional branches for convolution and channel attention calculation, we can make the features of the dual-branch no longer have obvious demarcation after the fusion block processing, so that the local and global information can be fully fused. In addition, this paper combines all the intermediate stage features additively before the image reconstruction module, and it is argued that in the deep image super-resolution network, with the deepening of the depth, the network will gradually discard the low-frequency features and retain the high-frequency features, but in fact, in the image restoration, both the low-frequency features and the high-frequency features should contain a certain amount of effective information. So to make full use of the low-frequency and high-frequency information, this paper chooses to combine the features of each stage, to maximally retain the information that is effective for recovering images.

In addition, to improve the model's ability to learn image features in the training phase and to reduce the computational effort in the inference phase, this paper adopts the design idea of repVGG [11] on the convolutional branch. The model makes the convolutional branch have three branches in each module in the middle by adding another 1×1 convolutional branch in addition to the residual link. This design increases the complexity of the model and can improve the model's learning of image features. In the inference stage of the model, the model then removes the redundant 1×1 convolutional branches, which allows the model to reduce the amount of computation in inference significantly and maintain a relatively stable image recovery performance.

Finally, in the model image reconstruction stage, this paper uses sub-pixel convolution to upsample the features which are widely used in this field.

The final results show that the performance of the model proposed in this paper is optimal for image recovery in comparison with other lightweight models.

In summary, the main work of this paper is:

(1) An innovative two-way fusion network of Convolution and Transformer is designed, which makes full use of the characteristics of the Convolution and Transformer branches using a two-way structure, effectively improving the limitations and

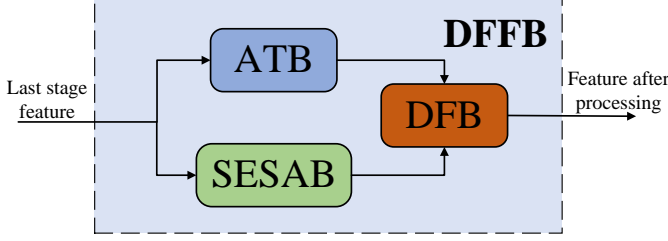


Fig. 3: Mechanisms for DFFB processing features

shortcomings of previous methods in extracting global features of the image, and significantly enhancing the performance of the lightweight super-resolution reconstruction model;

(2) An efficient convolutional network branch is constructed, which enables the branch to focus on extracting global coarse-grained information of the image and broader image context information through the orderly combination of deeply separable convolution and spatial self-attention computational modules;

(3) A novel multi-scale dual-path feature fusion block is constructed, which enables the dual-branch features to complement each other's information by splitting the input features multiple times and inputting them into multiple branches for convolution or channel attention computation followed by fusion, effectively integrating the image feature information from different architectural branches to achieve more detailed and accurate super-resolution reconstruction results;

(4) A new feature multiplexing module is designed, which retains the low and high-frequency information favourable to image recovery through the fusion of multi-stage features and further compensates for the high-frequency details that may have been lost in the above processing, thus enhancing the quality of image recovery.

II. RELATED WORKS

A. Lightweight Single Image Super-Resolution Algorithms

Dong et al [7]. proposed for the first time a single-image super-resolution model based on convolutional neural networks for low-resolution image recovery, called SRCNN (Super-Resolution Using Convolutional Neural Network). This model uses deep learning methods to process the recovery of low-resolution images for the first time and has achieved great success. After this, a large number of methods using deep learning and convolutional neural networks to deal with single-image super-resolution problems have appeared at home and abroad. For a general convolutional neural network model, as the number of layers and parameters increases, the expression ability and performance of the model get better. However, this way of improving model performance has its limitations because as the network size increases, a large number of parameters and computation costs will limit the deployment and training of the model on hardware devices. Therefore, to solve this problem, many lightweight approaches based on convolutional neural networks have emerged in the field of single-image super-resolution, including but not limited to the use of recursive structures [12], group convolution [13], etc.

to reduce the number of parameters and computation of the model. In this paper, some of the above methods are also used to reduce the number of parameters and computation of convolutional neural networks by using depth-separable convolution, which improves the performance and computational efficiency of the model.

B. Image Degradation Model

In single-image super-resolution studies, it is usually assumed that the low-resolution image is obtained from the high-resolution image through image degradation operations. It is thus assumed that the model can easily establish a mapping relationship between low-resolution images and high-resolution images of the same content, which also helps the subsequent supervised training. Based on this, the image recovery process of a single-image super-resolution model can be regarded as the inverse process of image degradation operation and also can be regarded as the process of mining the mapping relationship between low-resolution images and high-resolution images.

Image degradation [1] usually contains the following factors: downsampling, blurring, geometric transformation and noise. The high-resolution image is degraded by selecting one or a combination of these factors to obtain the corresponding low-resolution image. The downsampling method generally uses double and triple downsampling. Blurring is divided into motion blur and optical blur. Motion blur refers to the blur caused by the motion of the imaging device (e.g. camera, mobile phone) relative to the photographed object, while optical blur refers to simple Gaussian blur. Geometric transformations refer to the translation and rotation of an image. Noise, on the other hand, is classified according to the temporal distribution as Gaussian, gamma and exponential noise and other related noises.

Formulas can provide a brief overview of mass reduction operations:

$$y = H(x) + n = (x \otimes k) \downarrow_s + n \quad (1)$$

where $H(\cdot)$ is the degeneracy function and n denotes the noise. The degradation function $H(x)$ is obtained from a high resolution image x and a fuzzy kernel k . It is obtained by performing a convolution operation and then downsampling. The \downarrow_s indicates that the downsampling coefficient is s .

III. METHOD

In this paper, a new dual-way lightweight image super-resolution network based on the fusion of Transformer and convolutional neural network is proposed, and the main structure is shown in Fig. 2.

The network mainly contains the following modules: shallow feature extraction block (SFB: Shallow Feature Block), dual-way feature fusion block (DFFB: Double-way Feature Fusion Block), feature reusing block (FRB: Feature Reusing Block), and double-three times upsampling block (Upsample).

The model first makes the low-resolution image pass through a shallow feature extraction block, which consists of a 3×3 convolution and an ELU activation function, aiming

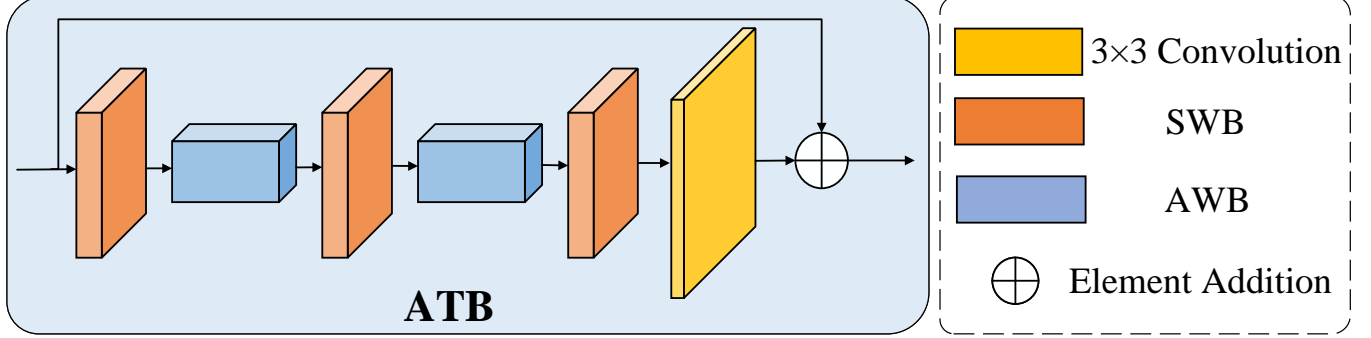


Fig. 4: ATB network architecture

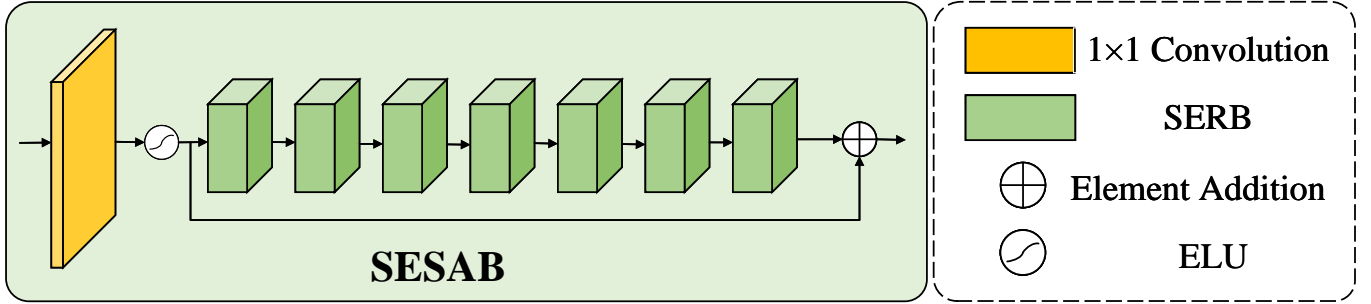


Fig. 5: SESAB network architecture

at first extracting the shallow feature map of the image at the very beginning stage, which is convenient for subsequent feature mining. Then the model passes the feature map through some two-way feature fusion blocks for feature extraction, and finally, several intermediate features obtained through the various stages of the DFFB in front of the final additive connection are merged and passed through the feature reuse module, to facilitate the full fusion of each intermediate feature to disrupt the information, and to carry out the subsequent information supplementation. Finally, the fully fused features are passed through the upsampling module for image reconstruction.

Assuming that the input low-resolution image is denoted as I_{LR} , shallow feature extraction is first performed on I_{LR} :

$$f_0 = \text{Conv}_{3 \times 3}(I_{LR}) \quad (2)$$

After that f_0 is fed into the feature extraction fusion block for feature extraction to get intermediate features for each stage:

$$f_n = \text{DFFB}(f_{n-1}), n = 0, 1, 2, 3 \quad (3)$$

Then each intermediate feature is spliced and input to the multiplexed feature fusion block to get the fused feature image:

$$f_4 = \text{FRB}(f_0 + f_1 + f_2 + f_3) \quad (4)$$

Finally, the fused image is then spliced with the shallow features and finally upsampled to get the reconstructed high-resolution image:

$$I_{HR} = \text{Upsample}(f_0 + f_4) \quad (5)$$

Next, this article will talk about the internal composition and operation mechanism of each block in detail to facilitate the understanding of the operation process of the network.

A. Double-Branch Feature Fusion Block Design

Firstly, there is the Dual-Feature Fusion Block (DFFB), whose main structure is shown in Fig. 3.

The DFFB module consists of three functional blocks, which are Axis Transformer Block (ATB: Axis Transformer Block), Space Enhanced Self-Attention Block (SESAB: Space Enhanced Self-Attention Block) and Double-Way Fusion Block (DFB: Double-Way Fusion Block).

Firstly, there is the Axis Transformer Block (ATB), whose main structure is shown in Fig. 4. In DFFB, the main role of the ATB module is to extract the local and regional features of the image. Through the self-attention mechanism, it establishes the regional dependency between image pixel points to better extract the local low-frequency information of the image.

Then there is the Space Enhanced Self-Attention Block (SESAB: Space Enhanced Self-Attention Block), whose main structure is shown in Fig. 5. The main role of this block in DFFB is to extract the global coarse-grained information of the image. This module helps the model to adaptively extract the critical information in the image and simultaneously weaken the non-critical information in the image during the training process through the stacking of depth-separable convolutional layers in a specific order and the combination of channel attention and spatial enhanced attention modules. This combination helps the model to efficiently extract the global coarse-grained information, which in turn compensates

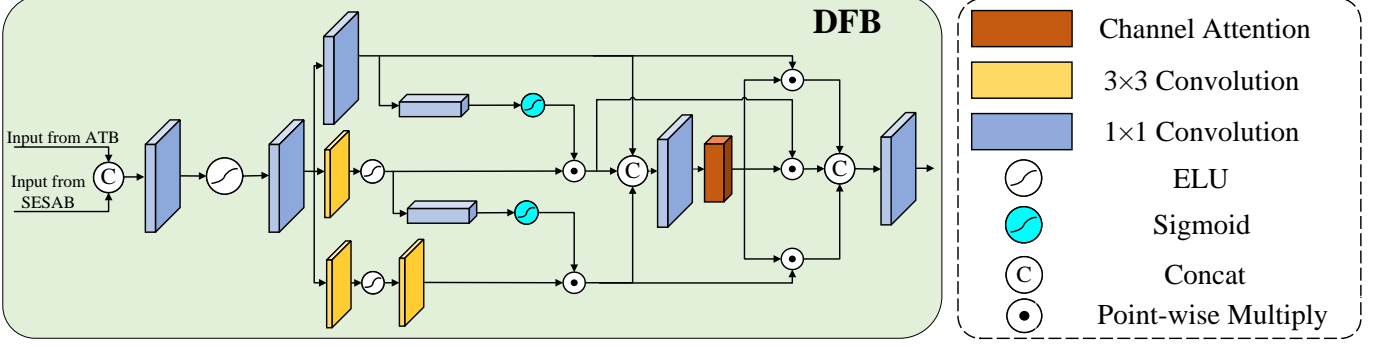


Fig. 6: DFB network architecture

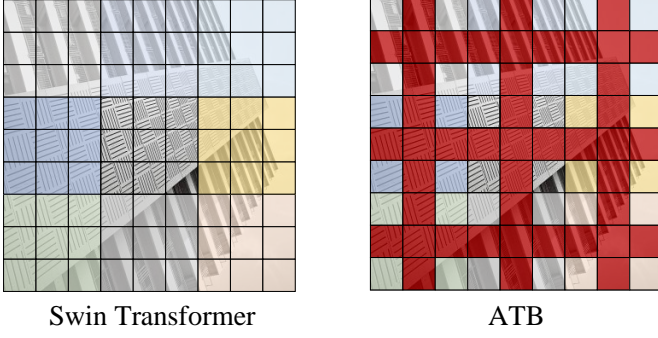


Fig. 7: Comparison of square-window self-attention calculation and axial-window self-attention calculation mechanisms

for the information in the branch where the ATB module is located.

Finally, there is the Double-Way Fusion Block (DFB: Double-Way Fusion Block), the main structure of which is shown in Fig. 6. From Fig. 3, we can know that after the feature map of the previous stage enters the DFB, it enters the ATB and SESAB respectively to be processed, and finally all the local area and global features extracted from the two branches are put into the DFB to be fused, and the information of its two branches is fully disrupted and mixed, and finally inputted into the next stage to be processed. Its formula can be expressed as follows:

$$f_i = DFB(ATB(f_{i-1}), SESAB(f_{i-1})) \quad (6)$$

Equation 6 indicates that the feature f_i of the i th stage is obtained from the feature f_{i-1} outputted from the previous DFB module after processing by ATB, SESAB module and then fused by DFB module.

1) *Axis Transformer Block*: The Swin Transformer model proposed by Liu et al [9]. has achieved great success in the field of computer vision, which achieves the effect of establishing long-distance dependence on the more distant pixels of an image by slicing the image, partitioning it into image blocks (Patch) with partial overlap, and then using a multi-layered square window to compute the self-attention between the blocks to achieve the effect of establishing long-distance dependence on the more distant pixels of the image. However, the model requires a larger number of network layers

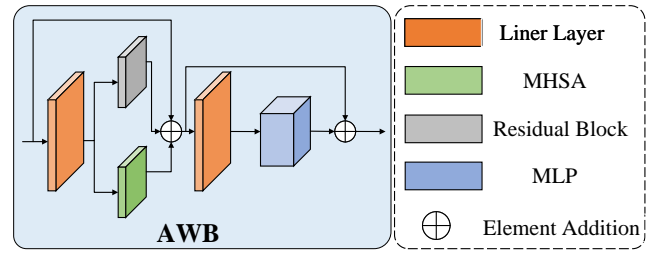


Fig. 8: AWB Block

to slice the image to achieve the effect of square windows moving across the graph, and thus the model requires a larger amount of computation to take advantage of its global modelling capabilities. Some previous works tried to reduce the number of layers of the Swin Transformer for feature extraction, but the experimental results found that once the number of layers of the Swin Transformer is reduced, the global feature extraction ability of the model will be greatly reduced, and it will be more biased towards extracting regional and local features of the image.

In order to solve the above problems, a new self-attention computational mechanism is used in this paper, as shown in Fig. 7.

This self-attention computational mechanism changes the shape of the self-attention window and uses an axial attention window (the red part) to compute the self-attention. The advantage of using an axial window is that the window can span multiple square windows, increasing the number of indirectly dependent pixels to be established while decreasing the number of pixels for which direct dependencies are computed, thus allowing the model to quickly establish global dependencies of pixels with fewer network layers.

Based on the axial self-attention computational mechanism of Fig. 7, this algorithm uses the Axial Transformer computational module to extract the image's regional and local features as shown in Fig. 4. Where AWB(Axis Window Block) module is the axial attention computing module and its internal structure is shown in Fig. 8. SWB(Square Window Block) module is the square window self-attention computing module with the same mechanism as Swin Transformer, and its internal structure is shown in Fig. 9. Both the AWB module and SWB module are self-attention computation modules constructed

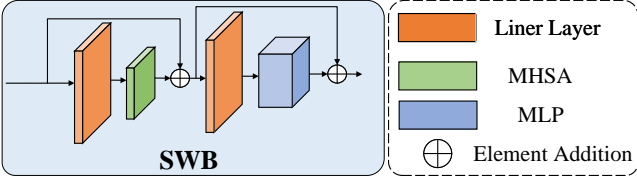


Fig. 9: SWB Block

using linear layers, fully connected layers, Multi-Head Self-Attention (MHSA: Multi-Head Self-Attention), and Residual Block. For the features f_i entering the AWB.

$$f_{i+1} = f_i + RB(LN(f_i)) + MHSA(LN(f_i)) \quad (7)$$

$$f_{i+2} = f_{i+1} + MLP(LN(f_{i+1})) \quad (8)$$

Finally, f_{i+2} is obtained as the output feature.

For the features f_i entering the SWB.

$$f_{i+1} = f_i + MHSA(LN(f_i)) \quad (9)$$

$$f_{i+2} = f_{i+1} + MLP(LN(f_{i+1})) \quad (10)$$

Finally, get f_{i+2} as the output feature. The method replaces the moving window mechanism of the Swin Transformer by designing the cross-computation of the axial attention window and square window, which drastically reduces the computation of the Transformer branch and efficiently establishes the long-distance indirect dependency between pixels.

2) *Space Enhanced Self-Attention Block*: In the design of the convolutional branch, this model refers to the construction of RCAN [14], by using the designed residual convolution block (SERB: Space Enhanced Residual Block) stacking to achieve the convolutional neural network on the image feature extraction. At the same time, in order to alleviate the rising number of model parameters due to the stacking of residual convolutional blocks, the part uses depth-separable convolution to do a lot of lightweight processing of residual convolutional blocks, and innovatively combines the spatial enhanced attention module (ESA: Enhanced Self-Attention) [15] and channel attention module (CA: Channel Attention) [16] at the end of each residual convolutional block, which is used to extract features from images by the convolutional neural network. Channel Attention, which is used to enhance the ability of the residual convolution block to extract image features, so that the residual convolution block can have the ability to extract the global coarse-grained features of the image, which is convenient for the subsequent supplementation of the feature maps processed by the ATB module.

The main structure of SERB is shown in Fig. 10:

Suppose the input features are f_i :

$$f_{i3} = ELU(GConv(DwConv(GConv(f_i)))) \quad (11)$$

$$f_{i+1} = ELU(f_i + Conv(f_i) + f_{i3}) \quad (12)$$

where f_{i3} denotes the feature map of the output of the third branch counting down from the top in SERB stage 1.

For stage 2, this paper uses $f_{(i+1)3}$ to denote the feature map of the output of the third branch counting down from the top in SERB stage 2, and so there is:

$$f_{(i+1)3} = ELU(GConv(DwConv(GConv(f_{i+1})))) \quad (13)$$

$$f_{i+2} = ESA(CA((f_{i+1} + Conv(f_{i+1}) + f_{(i+1)3}))) \quad (14)$$

Thus the output feature of the SERB is f_{i+2} .

In the construction process of the above SERB, the model uses the spatially enhanced attention module and the channel attention module. The main role of the channel attention module is to give each channel of the feature map a separate adaptive feature weight during the training process so that it can achieve the effect of weakening the invalid features and strengthening the important features by adaptively adjusting the feature weights during the training process, and improve the efficiency and quality of the model's image recovery. After processing by the channel attention module, the spatial enhancement attention module can further extract the global coarse-grained features of the image, thereby improving the effect of model pixel recovery.

B. Feature Reuse Block

When the depth of the network is deeper, it was examined during the experiments that the feature image loses some of the information that helps in image recovery as the training progresses in the deep network. Some previous studies have also shown that both shallow feature images and deep feature images have the same information that helps image recovery for reconstruction.

In view of the phenomenon that the quality of the reconstructed image is degraded due to the loss of information in the shallow layer of the feature image, a new feature reuse module is specially designed in this model before the image reconstruction stage. And this technique adopts the same mechanism as DFB, using four branches of progressive feature fusion to fully fuse the shallow features with the deeper features, fully mixing the useful information in the shallow feature map and the information in the deeper feature map that is beneficial to the image recovery, to achieve the maximisation of the efficiency of the image reconstruction and the minimisation of the loss of the feature information. The internal structure of the FRB module is shown in Fig. 11.

The model adds the intermediate feature images of the previous four stages in the learning process and then inputs them into the FRB module for the deep fusion and restructuring of the shallow features and the deep features, to avoid the loss of information in the training process as much as possible.

IV. EXPERIMENTS DETAIL

A. Dataset

1) *Training Dataset*: In this paper, we use the DIV2K image set [23], which is popular in the field of image super-resolution, as a training set, and use this dataset to train and validate the designed model. The dataset consists of 800 training images (image number: 1-800) and 100 validation

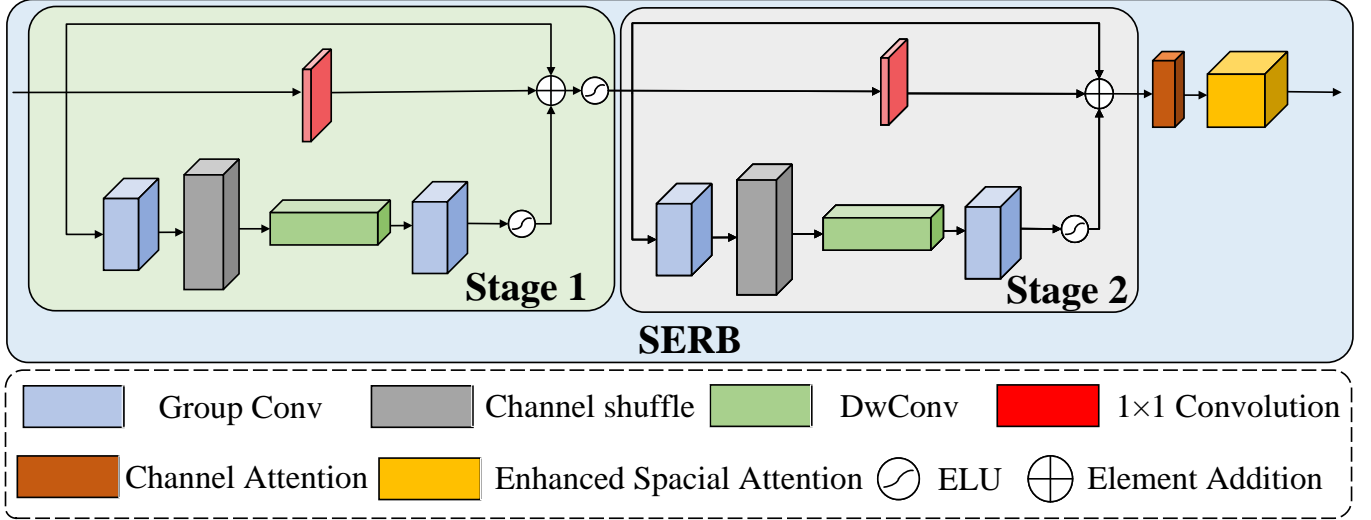


Fig. 10: SERB main framework

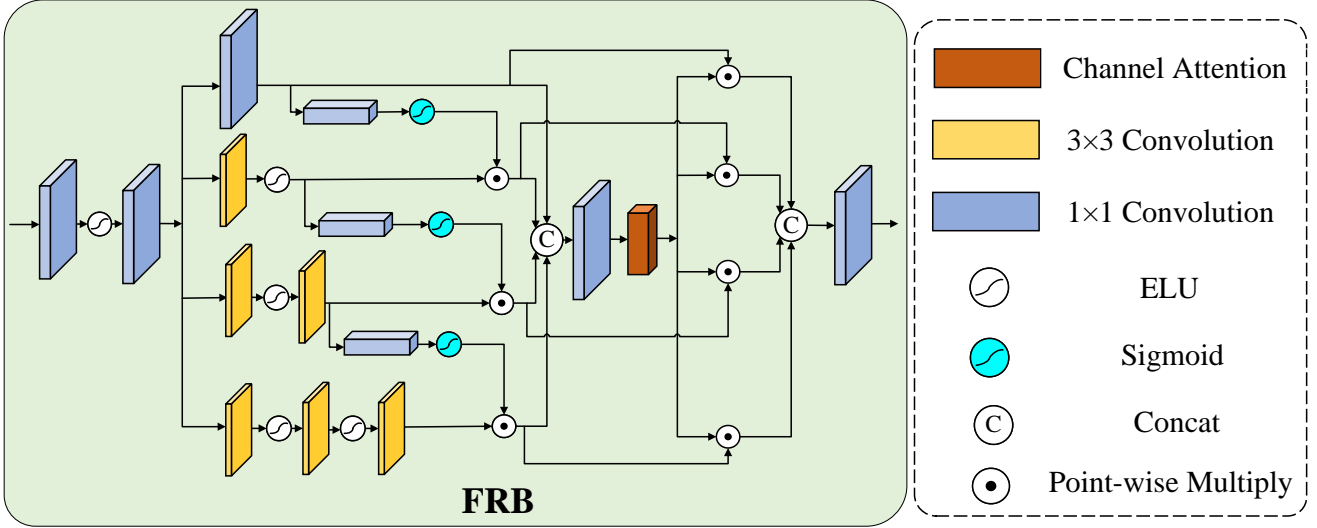


Fig. 11: FRB main framework

images (image number: 801-900). To facilitate quick validation during training and intermediate model saving according to the given rules, the model uses 10 of the validation images for actual validation during training (image numbers: 841-850). The model uses double-triple downsampling for the original HR images. In addition, in order to increase the complexity of the test images and the actual effect of the model after training, the experiment also used data augmentation on the training set to increase the difficulty of the model in learning the samples by randomly rotating the training set images by 90° , 180° , 270° , and horizontally flipping them to enhance the expressive ability of the model.

During training, the model with magnification of $\times 2$ is trained first, and after the $\times 2$ model is trained, the trained model is loaded as a pre-trained model onto the models with magnification of $\times 3$ and $\times 4$ for subsequent training.

2) *Test Dataset*: To ensure the objectivity of the comparison with other models, the following experiments are also validated using the five types of standard validation sets widely used in the field: Set5 [24], Set14 [25], B100 [26], Urban100 [27], and Manga109 [6]. To make a fair comparison with the previous models, the peak signal to noise ratio (PSNR: peak signal to noise ratio) and structural similarity index (SSIM: structural similarity index) are used as metrics for each test set, respectively, for the brightness (Y) channel in YCbCr space. signal to noise ratio (PSNR: peak signal to noise ratio) and structural similarity (SSIM: structural similarity index) as metrics, and the PSNR and SSIM values of each test set are calculated separately and compared.

B. Experimental Setup

During model training, 48 64×64 image blocks were randomly selected in each batch. Adam is used as the optimiser

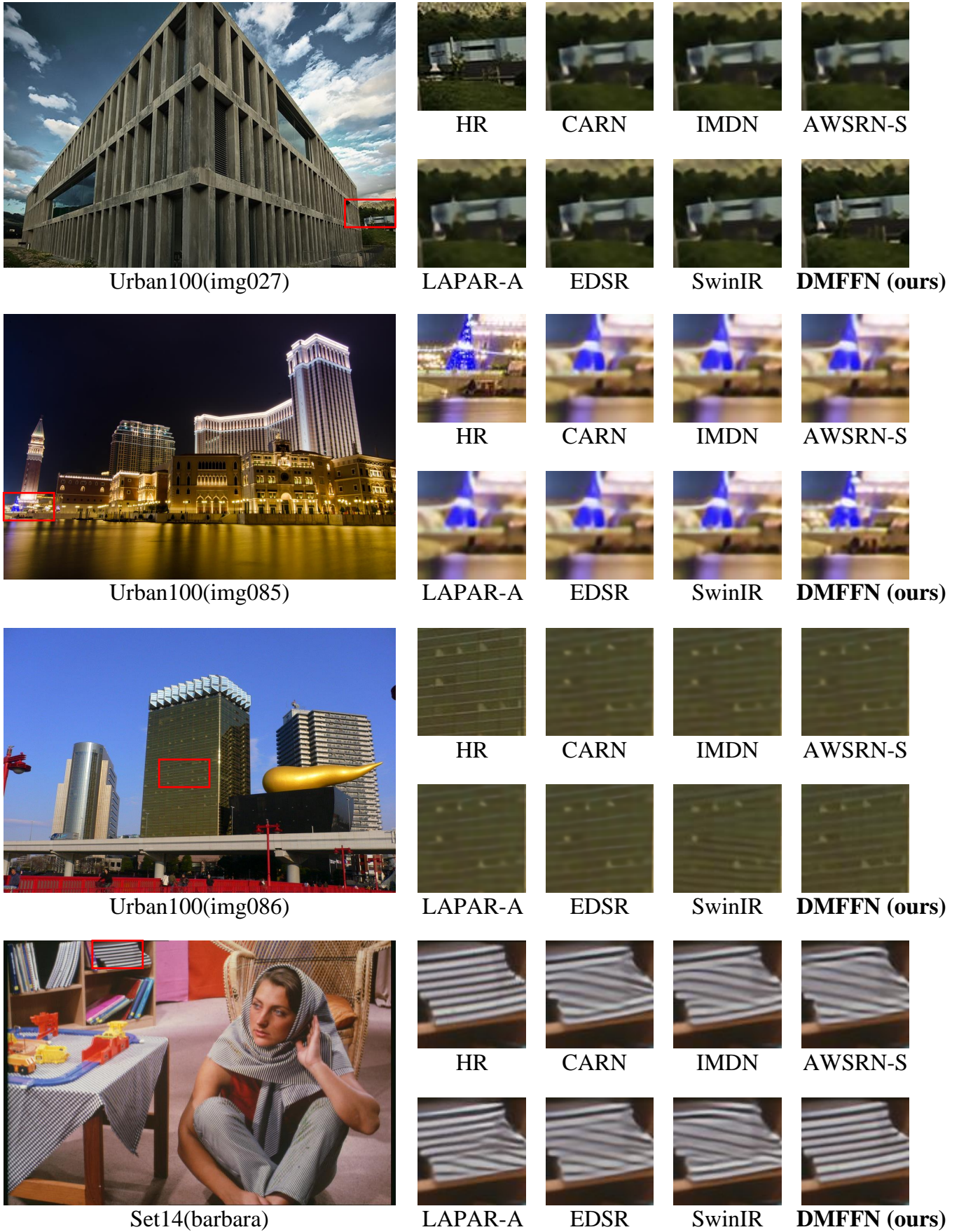


Fig. 12: Visual comparison of **bicubic image SR** ($\times 4$) methods.

TABLE I: Quantitative comparison (average PSNR/SSIM) with state-of-the-art methods for **lightweight image SR** on benchmark datasets.

scale	model	param(/K)	training set	Set5		Set14		BSD100		Urban100		Manga109	
				PSNR	SSIM								
$\times 2$	LatticeNet [17]	800K	DIV2K	38.1	0.9608	33.6	0.9177	32.21	0.9001	32.29	0.9297	38.81	0.9773
	AWSRN-M [18]	756K	DIV2K	38.06	0.9607	33.7	0.9187	32.2	0.8999	32.25	0.9288	38.94	0.9774
	MAFFSRN-L [19]	1063K	DIV2K	38.04	0.9605	33.66	0.9181	32.21	0.9	32.23	0.9294	38.66	0.9772
	SwinIR [20]	878K	DIV2K	38.14	0.9611	33.86	0.9206	32.31	0.9012	32.76	0.934	39.12	0.9783
	ELAN [21]	582K	DIV2K	38.17	0.9611	33.94	0.9207	32.3	0.9012	32.76	0.934	39.11	0.9782
	DLGSANet-tiny [22]	566K	DIV2K	38.16	0.9611	33.92	0.9202	32.26	0.9007	32.82	0.9343	39.14	0.9777
$\times 3$	DMFFN (ours)	669K	DIV2K	38.2	0.9613	33.87	0.9199	32.29	0.9011	32.76	0.9336	39.21	0.9782
	LatticeNet	765K	DIV2K	34.4	0.9272	30.32	0.8416	29.1	0.8049	28.19	0.8513	33.63	0.9442
	AWSRN-M	1143K	DIV2K	34.42	0.9275	30.32	0.8419	29.13	0.8059	28.26	0.8545	33.64	0.945
	MAFFSRN-L	807K	DIV2K	34.45	0.9277	30.4	0.8432	29.13	0.8061	28.26	0.8552	-/-	-/-
	EMASRN	437K	DIV2K	34.36	0.9264	30.3	0.8411	29.05	0.8035	28.04	0.8493	33.43	0.9433
	SwinIR	886K	DIV2K	34.62	0.9289	30.54	0.8463	29.2	0.8082	28.66	0.8624	33.98	0.9478
	ELAN	590K	DIV2K	34.61	0.9288	30.55	0.8463	29.21	0.8081	28.69	0.8624	34	0.9478
	DLGSANet-tiny	572K	DIV2K	34.63	0.9288	30.57	0.8459	29.21	0.8083	28.69	0.863	34.1	0.948
$\times 4$	DMFFN (ours)	708K	DIV2K	34.62	0.9293	30.48	0.8467	29.26	0.8094	28.78	0.8645	34.31	0.949
	LatticeNet	777K	DIV2K	32.18	0.8943	28.61	0.7812	27.57	0.7355	26.14	0.7844	30.54	0.9075
	AWSRN-M	1254K	DIV2K	32.21	0.8954	28.65	0.7832	27.6	0.7368	26.15	0.7884	30.56	0.9093
	MAFFSRN-L	830K	DIV2K	32.2	0.8953	28.62	0.7822	27.59	0.737	26.16	0.7887	30.33	0.9069
	EMASRN	558K	DIV2K	32.17	0.8948	28.57	0.7809	27.55	0.7351	26.01	0.7838	30.41	0.9076
	SwinIR	897K	DIV2K	32.44	0.8976	28.77	0.7858	27.69	0.7406	26.47	0.798	30.92	0.9151
	ELAN	601K	DIV2K	32.43	0.8975	28.78	0.7858	27.69	0.7406	26.54	0.7982	30.92	0.915
$\times 4$	DLGSANet-tiny	581K	DIV2K	32.46	0.8993	28.79	0.7871	27.7	0.7415	26.55	0.8033	30.98	0.9161
	DMFFN (ours)	765K	DIV2K	32.41	0.8981	28.74	0.7874	27.74	0.7421	26.67	0.8029	31.24	0.917

and $\beta_1 = 0.9$, $\beta_2 = 0.99$ is set. All models in this paper are set to 1,000,000 iteration cycles, and the learning rate is set to $2e - 4$ at the beginning and halved at the 50,000th, 80,000th, 90,000th, and 95,000th iterations. The loss function is set to the L1 loss function.

In this paper, we use the Pytorch framework, 2 Nvidia 2080Ti GPUs for model training and testing.

C. Results on Image SR

1) *Quantitative comparison*: In the objective evaluation index comparison, the experimental results were selected to compare the model test results of average PSNR and average SSIM with the magnification of $\times 2$, $\times 3$, and $\times 4$, as shown in Table 1. This comparison compares the present model with the classical models in the last three years. From the results, it can be seen that the tested values of average PSNR and average SSIM of the present model exceed the majority of the classical models and maintain a more excellent level. From the result, it can be concluded that the network architecture of the present model reaches the level of SOTA (State-Of-The-Art).

2) *Visual Comparison*: The images in the Set14 test set and the images in the Urban100 test set were selected as samples for the experimental results, as shown in Fig. 12. The original HR image, the model CARN [13], IMDN [28], AWSRN-S [18], LAPAR-A [29], EDSR [30], and SwinIR [20] were used as the control models to show the subjective effect of the model for image recovery. From the comparison, it can be seen that the model shows significant improvement in its effectiveness for image detail texture recovery. In the Barbara image, the model can easily distinguish the texture details in the diagonal upward direction, and can also clearly distinguish the distance for the thinly spaced stripes. In the img085 image, although the reconstructed image of this model still has some distance and blurring compared with the original HR image, compared with the restoration effect of other models, the model in this paper has richer and more realistic details in

the restoration of the distant light, and there is no problem of missing details, while the other images have varying degrees of missing details.

D. Ablation Study and Discussion

In this paper, we first remove the ATB branch and use the same structure as the residual convolution branch to replace the ATB branch, and use the two paths of the residual convolution combination to perform the extraction of low-resolution image features as well as image recovery, and the results of the image recovery are shown in the second row of Table II.

TABLE II: Ablation study on Two-Branch design

scale	SESAB	ATB	PSNR	SSIM
$\times 4$	w	w	31.24	0.9170
	w	w/o	30.37	0.9068
	w/o	w	30.55	0.9083

Afterwards, the experiment removes the SESAB branch and uses the same structure as the ATB branch to replace the residual convolutional branch, and uses the two pathways combined with the ATB branch to extract low-resolution image features for subsequent image recovery, and the results of image recovery are shown in the third row of Table II. The experimental results show that the hybrid two-way network model has better results than the two-way network with all Transformer branches and the two-way network with all Convolutional Neural Network branches.

TABLE III: Ablation study on DFB design

scale	DFB	PSNR	SSIM
$\times 4$	w	31.24	0.9170
	w/o	31.15	0.9164

The second set of experiments (Table III) examined the effect of the presence or absence of the DFB module on the effectiveness of image recovery for the network model. This experiment removes the DFB module and replaces it with the use of a convolution kernel for the convolution along the channels after splicing along the channel dimensions, compressing the feature map from 2C to C, and then proceeding to the feature extraction of the subsequent images. It can be seen that the two-way network with the DFB module can better fuse the feature information of the two branches to achieve better image super-resolution reconstruction.

TABLE IV: Ablation study on FRB design

scale	FRB	PSNR	SSIM
$\times 4$	w	31.24	0.9170
	w/o	31.03	0.9141

The third set of experiments (Table IV) examined the effect of the presence or absence of the FRB module on the image recovery results. In the experiments, the FRB module is removed and the convolution kernel is used for the convolution along the channels after splicing along the channel dimensions, and the final feature image is compressed from 4C to C, and then the subsequent image recovery is performed. It can be seen that the network with the FRB module is more capable of combining the information contained in the shallow and deep features to achieve better image recovery.

V. CONCLUSION

In this paper, a lightweight progressive multi-scale feature fusion network based on a two-brach convolutional neural network and Transformer is proposed. The main work of this paper is to design a two-way progressive feature multiscale fusion block that combines the spatially enhanced attention block to the traditional single-branch convolutional network and to fuse the local features of the image extracted by the Transformer branch with the coarse-grained global features extracted by the convolutional branch, to achieve the final information utilisation rate and the expressive ability of the model. The experimental results show that the method of this paper is effective, whether from the principle of algorithm design or specific objective experiments, it proves that the model is significantly better than the existing methods.

REFERENCES

- [1] Zhihao Wang, Jian Chen, and Steven CH Hoi. Deep learning for image super-resolution: A survey. *IEEE transactions on pattern analysis and machine intelligence*, 43(10):3365–3387, 2020.
- [2] Wenzhe Shi, Jose Caballero, Christian Ledig, Xiahai Zhuang, Wenjia Bai, Kanwal Bhatia, Antonio M Simoes Monteiro de Marvao, Tim Dawes, Declan O'Regan, and Daniel Rueckert. Cardiac image super-resolution with global correspondence using multi-atlas patchmatch. In *Medical Image Computing and Computer-Assisted Intervention-MICCAI 2013: 16th International Conference, Nagoya, Japan, September 22-26, 2013, Proceedings, Part III 16*, pages 9–16. Springer, 2013.
- [3] Keyan Chen, Wenyuan Li, Sen Lei, Jianqi Chen, Xiaolong Jiang, Zhengxia Zou, and Zhenwei Shi. Continuous remote sensing image super-resolution based on context interaction in implicit function space. *IEEE Transactions on Geoscience and Remote Sensing*, 61:1–16, 2023.
- [4] Matt W Thornton, Peter M Atkinson, and DA Holland. Sub-pixel mapping of rural land cover objects from fine spatial resolution satellite sensor imagery using super-resolution pixel-swapping. *International Journal of Remote Sensing*, 27(3):473–491, 2006.
- [5] Wilman WW Zou and Pong C Yuen. Very low resolution face recognition problem. *IEEE Transactions on image processing*, 21(1):327–340, 2011.
- [6] Yusuke Matsui, Kota Ito, Yuji Aramaki, Azuma Fujimoto, Toru Ogawa, Toshihiko Yamasaki, and Kiyoharu Aizawa. Sketch-based manga retrieval using manga109 dataset. *Multimedia tools and applications*, 76:21811–21838, 2017.
- [7] Chao Dong, Chen Change Loy, Kaiming He, and Xiaoou Tang. Image super-resolution using deep convolutional networks. *IEEE transactions on pattern analysis and machine intelligence*, 38(2):295–307, 2015.
- [8] Jinsu Yoo, Taehoon Kim, Sahaeng Lee, Seung Hwan Kim, Honglak Lee, and Tae Hyun Kim. Enriched cnn-transformer feature aggregation networks for super-resolution. In *Proceedings of the IEEE/CVF winter conference on applications of computer vision*, pages 4956–4965, 2023.
- [9] Ze Liu, Yutong Lin, Yue Cao, Han Hu, Yixuan Wei, Zheng Zhang, Stephen Lin, and Baining Guo. Swin transformer: Hierarchical vision transformer using shifted windows. In *Proceedings of the IEEE/CVF international conference on computer vision*, pages 10012–10022, 2021.
- [10] Xiangning Chen, Cho-Jui Hsieh, and Boqing Gong. When vision transformers outperform resnets without pre-training or strong data augmentations. *arXiv preprint arXiv:2106.01548*, 2021.
- [11] Xiaohan Ding, Xiangyu Zhang, Ningning Ma, Jungong Han, Guiguang Ding, and Jian Sun. Repvgg: Making vgg-style convnets great again. In *Proceedings of the IEEE/CVF conference on computer vision and pattern recognition*, pages 13733–13742, 2021.
- [12] Jiwon Kim, Jung Kwon Lee, and Kyoung Mu Lee. Deeply-recursive convolutional network for image super-resolution. In *Proceedings of the IEEE conference on computer vision and pattern recognition*, pages 1637–1645, 2016.
- [13] Namhyuk Ahn, Byungkon Kang, and Kyung-Ah Sohn. Fast, accurate, and lightweight super-resolution with cascading residual network. In *Proceedings of the European conference on computer vision (ECCV)*, pages 252–268, 2018.
- [14] Zudi Lin, Prateek Garg, Atmadeep Banerjee, Salma Abdel Magid, Deqing Sun, Yulun Zhang, Luc Van Gool, Donglai Wei, and Hanspeter Pfister. Revisiting rcan: Improved training for image super-resolution. *arXiv preprint arXiv:2201.11279*, 2022.
- [15] Jie Liu, Wenjie Zhang, Yuting Tang, Jie Tang, and Gangshan Wu. Residual feature aggregation network for image super-resolution. In *Proceedings of the IEEE/CVF conference on computer vision and pattern recognition*, pages 2359–2368, 2020.
- [16] Jie Hu, Li Shen, and Gang Sun. Squeeze-and-excitation networks. In *Proceedings of the IEEE conference on computer vision and pattern recognition*, pages 7132–7141, 2018.
- [17] Radu Alexandru Rosu, Peer Schütt, Jan Quenzel, and Sven Behnke. Latticenet: fast spatio-temporal point cloud segmentation using permutohedral lattices. *Autonomous Robots*, 46(1):45–60, 2022.
- [18] Chaofeng Wang, Zheng Li, and Jun Shi. Lightweight image super-resolution with adaptive weighted learning network. *arXiv preprint arXiv:1904.02358*, 2019.
- [19] Abdul Muqeet, Jiwon Hwang, Subin Yang, JungHeum Kang, Yongwoo Kim, and Sung-Ho Bae. Multi-attention based ultra lightweight image super-resolution. In *Computer Vision–ECCV 2020 Workshops: Glasgow, UK, August 23–28, 2020, Proceedings, Part III 16*, pages 103–118. Springer, 2020.
- [20] Jingyun Liang, Jiezhang Cao, Guolei Sun, Kai Zhang, Luc Van Gool, and Radu Timofte. Swinir: Image restoration using swin transformer. In *Proceedings of the IEEE/CVF international conference on computer vision*, pages 1833–1844, 2021.
- [21] Xindong Zhang, Hui Zeng, Shi Guo, and Lei Zhang. Efficient long-range attention network for image super-resolution. In *European conference on computer vision*, pages 649–667. Springer, 2022.
- [22] Xiang Li, Jiangxin Dong, Jinhui Tang, and Jinshan Pan. Dlgsanet: lightweight dynamic local and global self-attention networks for image super-resolution. In *Proceedings of the IEEE/CVF International Conference on Computer Vision*, pages 12792–12801, 2023.
- [23] Yawei Li, Yulun Zhang, Radu Timofte, Luc Van Gool, Lei Yu, Youwei Li, Xinpeng Li, Ting Jiang, Qi Wu, Mingyan Han, et al. Ntire 2023 challenge on efficient super-resolution: Methods and results. In *Proceedings of the IEEE/CVF Conference on Computer Vision and Pattern Recognition*, pages 1922–1960, 2023.

- [24] Marco Bevilacqua, Aline Roumy, Christine Guillemot, and Marie Line Alberi-Morel. Low-complexity single-image super-resolution based on nonnegative neighbor embedding. 2012.
- [25] Roman Zeyde, Michael Elad, and Matan Protter. On single image scale-up using sparse-representations. In *Curves and Surfaces: 7th International Conference, Avignon, France, June 24-30, 2010, Revised Selected Papers 7*, pages 711–730. Springer, 2012.
- [26] David Martin, Charless Fowlkes, Doron Tal, and Jitendra Malik. A database of human segmented natural images and its application to evaluating segmentation algorithms and measuring ecological statistics. In *Proceedings eighth IEEE international conference on computer vision. ICCV 2001*, volume 2, pages 416–423. IEEE, 2001.
- [27] Jia-Bin Huang, Abhishek Singh, and Narendra Ahuja. Single image super-resolution from transformed self-exemplars. In *Proceedings of the IEEE conference on computer vision and pattern recognition*, pages 5197–5206, 2015.
- [28] Zheng Hui, Xinbo Gao, Yunchu Yang, and Xiumei Wang. Lightweight image super-resolution with information multi-distillation network. In *Proceedings of the 27th ACM international conference on multimedia*, pages 2024–2032, 2019.
- [29] Wenbo Li, Kun Zhou, Lu Qi, Nianjuan Jiang, Jiangbo Lu, and Jiaya Jia. Lapar: Linearly-assembled pixel-adaptive regression network for single image super-resolution and beyond. *Advances in Neural Information Processing Systems*, 33:20343–20355, 2020.
- [30] Bee Lim, Sanghyun Son, Heewon Kim, Seungjun Nah, and Kyoung Mu Lee. Enhanced deep residual networks for single image super-resolution. In *Proceedings of the IEEE conference on computer vision and pattern recognition workshops*, pages 136–144, 2017.